inert fraction of the O_2/H_2 vehicle, a given warhead weight reduces its performance more severely than that of a nuclear vehicle.

Observations and Concluding Remarks

When warhead kill radius r is several hundred miles or more as assumed here for nuclear radiation against a manned target, then there exist three regions in intercept time-distance ($t - X_{Tt}$) space, each of which calls for a different class of interceptor. When $X_{Tt} < r$ (a few hundred naut miles) and required t is small ($\lesssim$100 sec), an all-warhead, nonpropulsive interceptor (i.e., a "space mine") may be indicated. For intermediate distances and allowable times, some optimal combination of warhead and maneuvering propulsion is required; for an O_2/H_2 interceptor having $F/W_0 = 1$, this combination region extends to $\sim$2000 naut miles and $\sim$500 sec. For larger X_{Tt} and t the all-propulsive interceptor is preferred. Although some shifting of these regions can be expected if r, F/W_0, and the propulsion method are varied, the foregoing values do not appear to be strong functions of any of these variables.

Solid propulsion is competitive only for very short intercept times where high acceleration can be decisive and where large nuclear bursts are ruled out for operational reasons. Oxygen-hydrogen propulsion is preferable throughout the intermediate range and up to $\sim$20,000 naut miles and 4000 sec; nuclear propulsion is preferable beyond these values. For example, an extrapolation from Fig. 2 reveals that where a warhead weight fraction of 0.1 is required in the "all-propulsive" case, then for $X_{Tt} \simeq$ 200,000 naut miles and $t \simeq$ 20,000 sec, a nuclear interceptor can cover nearly four times the volume of the given O_2/H_2 interceptor.

References

[1] "Military Space Operations 1975–1995," Vol. II, Rept. NDS-13, Nov. 1969, Aerojet-General Corp., Sacramento, Calif.

[2] Glasstone, S., ed., *The Effects of Nuclear Weapons*, U. S. Government Printing Office, April 1962.

Ocean-Height Measurement by Satellite Altimetry

J. G. MARSH*
Goddard Space Flight Center, Greenbelt, Md.
AND
B. C. DOUGLAS†
Wolf Research & Development Corporation, Riverdale, Md.

Introduction

SATELLITE altimeter experiments fundamentally represent a new way of gathering geodetic data. Because of this newness, very accurate orbits must be obtained for evaluation and use of the altimeter. Although this does not entirely preclude the use of altimeter data to determine the orbit, much more satisfactory and error-free analyses will be obtained if other tracking systems and methods are used for definitive determination of satellite position. The altimeter data can then be regarded as measurements from a known spacecraft position to the surface. This paper is concerned only with the accuracy attainable by dynamic long-arc orbit determination techniques. Other techniques such as short arcs and geometric determinations have not been treated.

A low inclination is favorable for a new geodetic satellite for several reasons. First, it is well known that present determinations of the zonal harmonics of the geopotential are deficient because of a lack of satellite data of geodetic quality with inclination below 30°. Second, the effect of longitude-dependent variations of the geopotential is generally reduced at low inclination, particularly in regard to resonance.[1] Since a resonance with a beat period of at least 2 days is always present, an inclination that minimizes resonance is a helpful factor.

The orbit determination requirements of satellite altimetry are severe. The separation of the geoid and the spheroid hardly reaches 100m. To be useful, measurement errors will have to be far smaller than this figure. Indeed, the nominal accuracy of the altimeter is planned to be 5m. The purpose of our investigation was to estimate the effect of model errors on the determination of satellite radial distance to see if the orbit determination requirements can be met and the altimeter accurately evaluated. Our results were obtained by simulation of least-squares solutions including the effect of model and instrument error in addition to random noise. The results show that if careful attention is given to scheduling of observations, orbits of the required accuracy can be obtained.

Tracking Systems

We considered tracking with STADAN optical, Unified S-Band (USB) radar, C-Band radar, and SAO Baker-Nunn optical systems. Figure 1 shows the positions of these instruments on a world map. In the case of the C-Band radars, we have studied only a partial system with, however, worldwide coverage.

The USB and SAO Baker-Nunn systems give excellent coverage of low inclination orbits whether inclined at $i = 20°$ or $i = 30°$. However, at $i = 20°$, the STADAN optical system is degraded, and certain important C-Band stations, e.g., Wallops Station, can no longer track. However, some STADAN and C-Band sites will be able to observe and will supplement previous GEOS analyses. A large amount of STADAN optical data is available for GEOS-I and II. These data plus SAO Baker-Nunn tracking data have been used with success to determine the locations of the STADAN optical stations. For the system as a whole, the center of mass position errors are 10m or less.[2] A third well-observed geodetic satellite would enable us to reduce this figure for some stations when the data is combined with data from GEOS-I and II.

Tracking Accuracy Studies

We analyzed (see Appendix) the error effects listed in Table 1 on the determination of the geocentric distance of a

Table 1 Tracking systems and model errors assumed for error analyses

Type	Frequency, min^{-1}	Data noise	Data bias	Station position error, m
SAO Baker-Nunn	10[a]	2 arcsec	none	20[c]
STADAN Optical	10[a]	2 arcsec	none	20
C-Band	60	5 m	2 m	20
Unified S-band-range	10	10 m	40 m[b]	20
USB range-rate	10	1 cm/sec	none	20

Gravity model error: SAO M1-SAO COSPAR (1969) to (8, 8) +20% error in resonant coefficients
GM error: 1:10^6

[a] Flash data, one sequence per pass.
[b] This bias is about 2½ times the normal uncertainty (see text).
[c] 10 m survey, 10 m center of mass.

Received October 26, 1970; revision received February 11, 1971. The ORAN computer program was designed and developed by C. F. Martin.

* Mathematician.

† Manager, Satellite Geodesy Section.

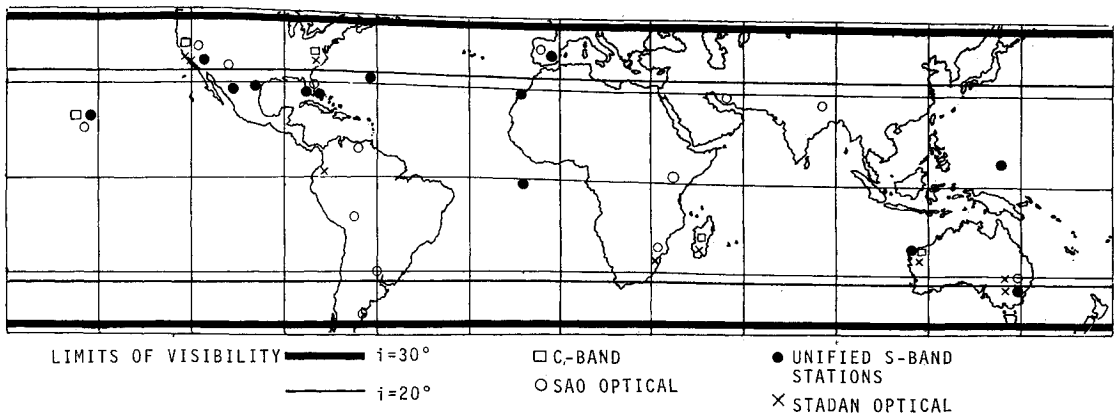

Fig. 1 Station visibility map.

low inclination, near-circular satellite orbit of period = 112 min. The optical data rates shown assume that the satellite has flashing lights. We have considered two orbits, one inclined at $i = 20°$, the other at $i = 30°$. The results relating to gravity model error, station coordinate error and tracking system errors except data coverage are quite general for orbits in the range of 10–40°. The major difference, as seen in Fig. 1, is one of coverage.

The tracking systems studied are known to have low noise and small biases. We chose the unrealistically large bias of 40m (normal biases are on the order of 15–20m) for the USB system only to evaluate the effect of a large bias on a system capable of dense tracking. In spite of such a large assumed bias, the most important sources of error were found to be the gravity model and station position uncertainty.

For the effects of gravity model error, we considered resonant and nonresonant terms separately. The estimate of the error of the nonresonant part of the geopotential was taken to be the difference between the SAO M1[3] and SAO COSPAR[4] models to (8, 8). The results obtained in Ref. 2 indicate that this estimate of error is probably pessimistic. The error in the 13-order resonant coefficients was taken to be 20% of their value. This is also pessimistic, but in any case, it has been found that resonance is no problem at i near 20°. The effect of resonance drops off dramatically at $i < 45°$[1] and might be further minimized by choosing a small beat period. Also, the effect of resonance radially is small.[5]

Because of model errors, there exists a definite limitation on the length of data arc that can be used. From our studies, we found 1-day solutions to be generally superior to either 12-hr or 5-day solutions. Twelve-hour solutions may suffer from lack of data, particularly for tracking systems with poor geographic distribution. In contrast, longer arcs have a more difficult time accommodating model error. Exceptions exist in that good results are sometimes available for short arcs if there is very intensive tracking, as will be seen below.

Figure 2a shows the total radial (and therefore altitude) error that can be expected from model error and noise for a typical 1-day STADAN optical solution. In this and all cases, gravity model errors other than resonance are by far dominant, although station error effects occasionally reach 5m. At $i = 20°$, the altitude error occasionally reaches nearly 30m. The situation is improved for $i = 30°$ because of better coverage by the tracking system; 10m is a typical figure, with excursions to 15 or 20m. The periods of the error curves are relatively large, exceeding 1 hr. Since the satellite is moving 3°/min, passage over small regions such as the Puerto Rican trench will yield good relative (and hence profile) measures even though the absolute error may be large.

Figure 2b shows that the radial error to be expected with USB tracking is worse at 30° than at 20° due to geometry; there was less tracking at $i = 30°$ than $i = 20°$. The importance of good scheduling is underscored. We can conclude that at $i = 20°$ or 30°, height error with USB tracking could be 10m on the average, with a variation of about 5–20m.

Figure 2c shows the performance of the partial C-Band system consisting of Hawaii, Western Test Range, Wallops Station, Winkfield, Madagascar, and Carnavon. This very sparse system can have periods of many hours in a day where

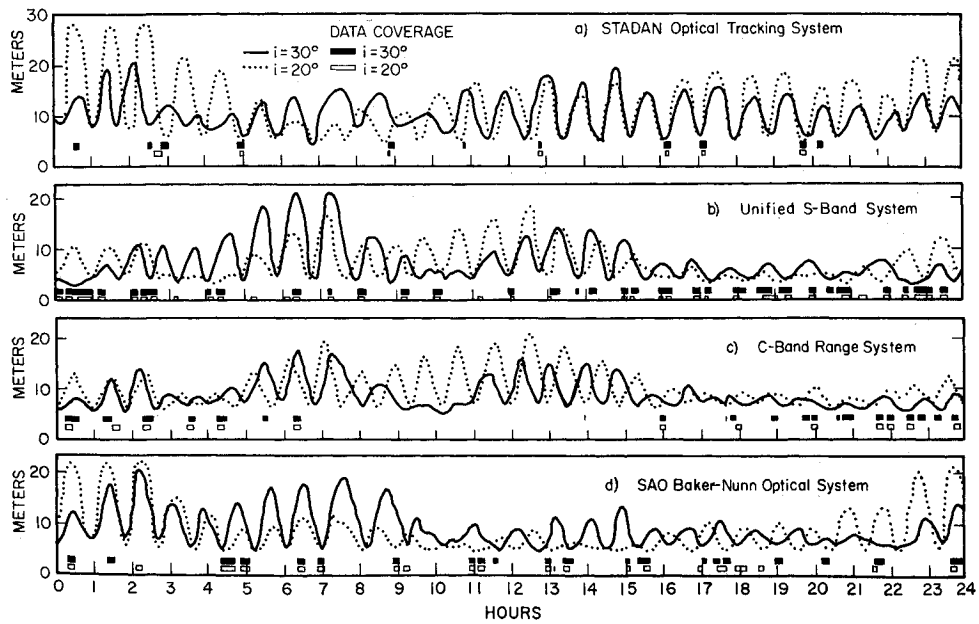

Fig. 2 Total radial error for a one-day orbital solution.

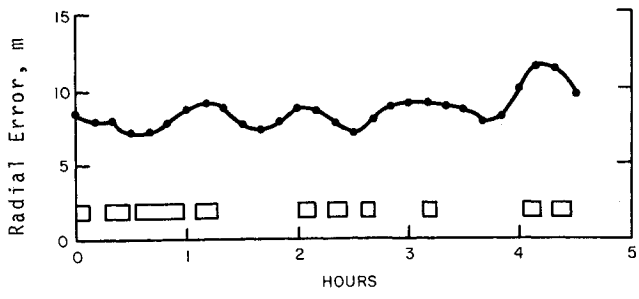

Fig. 3 Total radial error for a 4½-hr orbital solution, United S-Band System; inclination = 20°, □ = data coverage.

there is no tracking as in Fig. 2c, but the quality of the solution is still very high because of the accuracy of the data. These five C-Band stations do nearly as well as the 14 USB stations. Again, an average error of 10m with excursions to perhaps 20m will be seen. Even better results would be obtainable with more C-Band instruments. An error analysis was performed combining the STADAN optical and C-Band systems, but the results were not substantially improved. The C-Band data are so numerous and accurate, that optical data have low weight in a combined solution.

Figure 2d shows the case for the SAO Baker-Nunn system; again, errors of 10m are typical, with excursions to 20m.

All of the systems thus exhibit similar performance, because with modern tracking systems, observation noise is almost never a factor. Model error effects are generally one to three orders of magnitude more important than random noise.[6] It makes little difference whether a tracking system takes 10 or 100 observations in a pass over a tracking station. The position error tends to be minimized over the stations, as can be seen in Fig. 2, and the orbit is allowed to balloon out elsewhere. Occasionally, however, the relative geometry of the satellite orbit and the tracking system is such that nearly continuous coverage is obtained, at least for large segments of an orbit. Such was the case for the first 4-½ hr of simulated USB tracking for Fig. 2b. Simulating a solution over this period alone shows (Fig. 3) that the variation of the radial error is sharply reduced because the orbit is tightly constrained by the data nearly everywhere.

Although the maximum errors are of the order of 10m, the rate of change of error for the 4-½ hr orbit is much smaller than for the one-day orbit shown in Fig. 2c.

Conclusions

Assuming model errors that are probably pessimistic, we conclude from the foregoing that determination of absolute spacecraft altitude to better than 10m as an average will be difficult. This error can change as fast as 1m/2 min in areas with little or no tracking. In cases where tracking is intensive, the rate of change of the radial error can drop to 1m/30 min or less. Such errors are tolerable for surveys of the variation of ocean height.

Appendix: Error Analysis

The ORAN (Orbital Analysis) computer program used for this study was designed for computing the effects of random and systematic errors on minimum variance orbit determinations. Systematic errors can be in the form of either adjusted or unadjusted parameters, with the effects of the latter broken down into effects of the individual error sources. The program computes the effects of the unadjusted parameters on both the recovered parameters and the orbit, with the orbital effects propagated from epoch to any desired prediction time.

Mathematically, the unmodeled error propagation is based on the following observations. The minimum variance orbit determination uses the basic equation

$$\delta 0 = A\delta a + e \tag{A1}$$

to relate discrepancies ($\delta 0$) between measured and calculated observations to discrepancies (δa) between true and a priori estimates of the set of parameters to be recovered. The set δa includes the six orbital elements but may also include other parameters. The matrix A is the set of partial derivatives of the measurements with respect to the adjustable parameters, and e is a vector of measurement noise. When the least-squares criterion is used to solve Eq. (A1) for the best estimate of a, the result is

$$\delta\hat{a} = (A^TWA)^{-1}A^TW\delta 0 \tag{A2}$$

where W is the matrix of measurement weights. For the solution to be minimum variance, the weight matrix must be chosen such that $W^{-1} = E(ee^t)$. That is, W must be the inverse of the variance-covariance matrix of measurement noise. In the normal data reduction process, W is generally so chosen because it actually is measurement random error, in which case W is rather accurately expressed as a diagonal matrix.

For various reasons, the set of parameters adjusted in data reduction programs is only a subset of those parameters having some error. For example, our knowledge of geopotential coefficients is by no means complete. Yet a truncated model is always (of necessity) used, and the error in the coefficients used is ignored in all variance computations. Because the net effect is that e is not random, we can obtain a more accurate representation of the measurement discrepancy vector by expressing e as $e = K\gamma + \epsilon$, where γ is a set of errors in parameters previously ignored, K is the matrix of partial derivatives of the measurements with respect to these parameters, and ϵ is the vector of measurement random noise upon which W is still based. Substitution of this expression into Eq. (A1) gives

$$\delta 0 = A\delta a + K\gamma + \epsilon \tag{A3}$$

If the weight matrix for the measurements is based on ϵ and is the same as that used in the data reduction program, it follows that the solution for $\delta\hat{a}$ actually being obtained is not that given by Eq. (A2), but is a biased solution given by

$$\delta\hat{a} = (A^TWA)^{-1}A^TW(\delta 0 - K\gamma) \tag{A4}$$

From this relation, we may obtain by differentiation the effects of unit values of the set of Σ parameters;

$$\partial\delta\hat{a}/\partial\gamma = -(A^TWA)^{-1}A^TWK \tag{A5}$$

It follows that if the matrix K can be obtained, the effects of unit values of the γ parameters are obtained by substituting K for the $\delta 0$ vector used in the data reduction program. A priori estimates of errors in the γ parameters lead to an estimate of the magnitudes of the effects on recovered parameters, and the trajectory, of each γ parameter.

Uncertainties in the γ's are generally uncorrelated. If their correlations are known or can otherwise be accounted for, an estimate of the total or over-all accuracy of the orbital solution is readily obtainable. For this study, errors in station locations, GM, and the geopotential were considered.

References

[1] Douglas, B. C. and Palmiter, M. T., "An Analysis of Eccentric Deeply Resonant Orbits for Geodesy," *Journal of the Astronautical Sciences*, Vol. 17, No. 6, May–June 1970, pp. 313–336.

[2] Marsh, J. G., Douglas, B. C., and Martin, C. F., "NASA STADAN, SPEOPT and Laser Tracking Station Positions Derived from GEOS-I and GEOS-II Precision-Reduced Optical and Laser Observations," paper a.11, COSPAR, Leningrad, USSR, May 1970; to be published, 1971.

[3] Lundquist, C. A. and Veis, G., "Geodetic Parameters for a 1966 Smithsonian Institute Standard Earth," Special Report 200, Vol. 1, 1966, Smithsonian Astrophysical Observatory, Cambridge, Mass.

[4] Gaposchkin, E. M., "Improved Values for the Tesseral Harmonics of the Geopotential and Station Coordinates," *Dynamics of Satellites*, 1969, edited by B. Morando, Springer-Verlag, Berlin, 1970, pp. 109–118.

[5] Gedeon, G. S., Douglas, B. C., and Palmiter, M. T., "Resonance Effects on Eccentric Satellite Orbits," *Journal of the Astronautical Sciences*, Vol. 14, No. 4, July-August 1967, pp. 147–157.

[6] Douglas, B. C., Martin, C. F., Williamson, R. G., and Wagner, C. A., "Error Analyses of Resonant Orbits for Geodesy," *Celestial Mechanics*, Vol. 1, 1969, pp. 252–270.

Buckling of Axially Compressed, Core-Filled Cylinders with Transverse Shear Flexibility

CHARLES W. BERT*
University of Oklahoma, Norman, Okla.

Nomenclature

D_{qx}	=	transverse shear rigidity of shell in meridional plane (= KGh)
D_x	=	shell flexural rigidity in axial direction
E,E_c	=	elastic moduli, isotropic shell and core, respectively
E_x,E_y	=	elastic moduli of shell in axial and circumferential directions
F_0,F_1	=	dimensionless factors defined in Eqs. (21) and (19)
G	=	shear modulus of shell material in meridional plane
h	=	shell wall thickness
I_0,I_1	=	modified Bessel functions of orders zero and one
K	=	shear correction factor for shell wall ($=\frac{5}{6}$ for homogeneous shell; = 1 for shear-flexible sandwich shell)
k	=	core spring constant, defined by Eq. (3) and calculated by Eq. (4)
L	=	length of shell
m	=	$\pi m_1/L$; m_1 = number of axial half waves in buckle waveform
N	=	axial compressive force on shell only
N_{cr}	=	critical value of N at which buckling occurs
$\bar{N}_{cr},N_{cr}{}^*,N_{cr}{}^0$	=	special values of N_{cr}, Eqs. (14–16)
P_{cr}	=	critical value of total axial compressive force
p	=	normal pressure at core/shell interface due to elastic interaction
Q_0	=	amplitude of Q_x
Q_x	=	transverse shear stress resultant acting on face cut by position x
R	=	radius of shell middle surface; $\bar{R} = mR$
w	=	shell displacement normal to its middle surface
w_0	=	amplitude of w
x	=	axial position coordinate
λ	=	$1 - \nu^2$
ν,ν_c	=	Poisson's ratios, shell and core materials, respectively
Φ_1	=	Seide's core stiffness parameter
Ψ_0	=	$I_1(\bar{R})/I_0(\bar{R})$

Introduction

THE problem of axial-compression buckling of circular cylindrical shells containing a soft elastic core is important in the design of solid-propellant rocket-motor cases[1] and of foam-plastic cylinders foamed against a metal mold.[2] Numerous linear, small-deflection analyses of this problem have been performed for thin-walled isotropic cylinders.[3–6] Seide[5] and Yao[6] have shown that the presence of a core results in lower buckling loads for the axisymmetric mode than the unsymmetric ones. As in the case of unfilled cylindrical shells, experimental buckling loads for core-filled cylinders fall much lower than the prediction by linear buckling analysis.[5] However, the discrepancy decreases with increasing values of a dimensionless parameter Φ_1, which is proportional to E_c/E, the core-to-shell elastic modulus ratio. For example, for $\Phi_1 = 0$ (i.e., $E_c = 0$), the ratio of experimental buckling loads to analytical buckling loads averaged ~40%, while at $\Phi_1 = 0.25$, it averaged ~75%. Nonlinear, finite-deflection analyses have been found to serve as a lower bound to the experimental results.[7–8] Yao[6] has concluded that the interfacial shear stresses at the core/shell junction can be neglected, as was done in other analyses of this problem.

Apparently the only buckling analyses of a core-filled orthotropic shell is due to Lemke[9] and Holston.[10] They considered a specially orthotropic shell, but neglected transverse shear flexibility. However, it has been demonstrated that transverse shear flexibility is much more significant in composite-material structures than in homogeneous, isotropic ones of the same dimensions.[11]

The foregoing analyses modeled the core behavior either as a simple Winkler foundation or as a homogeneous, isotropic elastic continuum. Recently Myint[12] treated the problem using Pasternak's two-parameter foundation model, which is equivalent to a Winkler foundation with shear interaction. However, the effect of the second parameter was very weak. (This is consistent with Yao's findings on interfacial shear stress as described previously.)

The purpose of the present Note is to determine the effect of transverse shear flexibility on the buckling loads of core-filled specially orthotropic and isotropic cylinders.

Hypotheses

The following hypotheses form the bases for the analysis:

H1) Displacements are small compared to the shell thickness h and the core radius, so that the strain-displacement relations may be assumed to be linear.

H2) $h/R \ll 1$, where R is the radius of the shell middle surface.

H3) The effect of transverse shear flexibility is included in the same manner as used by Timoshenko[13] for beams and Reissner[14] for plates, i.e., shear distortion is included by use of an appropriate shear factor and transverse normal flexibility is neglected.

H4) The shell is assumed to behave macroscopically as an homogeneous, specially orthotropic, linearly elastic material.

H5) The core is assumed to be represented by an homogeneous, isotropic, linearly elastic continuum, which is related to a Winkler-type foundation by the analysis in Appendix A of Ref. 5.

H6) Only axisymmetric buckling modes are considered, since they are usually predominant in core-filled shell buckling.[5]

H7) Shear stress interaction between the shell and core at their interface is neglected.[6]

H8) Thermal, viscous, and dynamic effects are negligible.

Hypothesis H1 is justified for sufficiently high values of core stiffness. Hypotheses H2 and H3 call for a shell theory analogous to Love's first-approximation theory[15] with transverse shear flexibility added. However, for the axisymmetric case considered here, the Love first-approximation theory is identical to the improved first-approximation theory developed by Sanders.[16] The shell theory used here also is analogous to the Reissner theory of sandwhich shells.[17]

Hypothesis H4 includes isotropic materials as a special case and is approximately applicable to laminated composite

Received October 30, 1970.

* Professor, School of Aerospace, Mechanical and Nuclear Engineering. Associate Fellow AIAA.